

Oxidative Dehydrogenation of Ethylbenzene over $\text{Sm}_2\text{O}_3\text{-V}_2\text{O}_5$ System

Sankaran Sugunan* and Neeroli Kizhakayil Renuka

Department of Applied Chemistry, Cochin University of Science and Technology, Kochi 682 022, India

(Received July 23, 2001)

$\text{Sm}_2\text{O}_3/\text{V}_2\text{O}_5$ catalysts were synthesized by wet impregnation of samaria with an aqueous solution of ammonium trioxovanadate(V). The characterization of the prepared samples was carried out using EDX, XRD, FTIR and TG-DTA as well as a measurement of the surface area and pore volume. The catalysts were found to be stable up to 800 °C. Both amorphous and crystalline vanadate species were detected in the supported system. Vanadia species became anchored to the surface through an interaction with basic hydroxy groups and Lewis acid sites of the surface. Lewis acid and base sites decreased upon vanadia addition along with a concomitant enhancement of Brønsted acid sites. The oxidative dehydrogenation of ethylbenzene was carried out over Sm/V catalysts, which exhibited a styrene selectivity > 80%. The active species present in the supported system was concluded to be amorphous vanadia in tetrahedral coordination. The higher vanadia-loaded systems exhibited constant styrene selectivity, where crystalline tetraoxovanadates were predominantly formed.

Modern technology is searching for efficient catalytic processes that either eliminate or minimize the production of unwanted chemicals, giving emphasis to selectivity along with catalytic activity. In recent years, supported vanadia catalysts have attracted much attention, which boast wide applications in the area of partial or selective oxidation reactions of industrial importance. A large number of research work has been devoted to provide insight into the nature and reactivity of supported vanadia catalysts. The nature of the selected support material plays a crucial role in determining the active vanadia species. i.e., its chemical composition, crystallographic modification, morphology, and textural properties. Other parameters, such as preparation method and catalyst pretreatment, also influence the physical and chemical properties of the resulting catalysts. A preferential formation of compounds was observed on basic supports, whereas acidic supports favored V_2O_5 crystallites.^{1,2} Reactions catalyzed by supported vanadia systems include the oxidation of hydrocarbons,^{3,4} the ammoxidation of aromatics⁵ and the selective catalytic reduction of nitrogen oxides.⁶ Earlier studies have established that metal oxides, which are more acidic than vanadia, favor the formation of acidic products, whereas oxidative dehydrogenation reactions, which produce basic substances, proceed well on systems of basic oxides when supported with vanadia.⁷

Even though catalyst systems containing vanadia have been extensively studied, little attention has been paid to rare earth-supported vanadia analogues. In the present paper, we report on the synthesis and characterization of samaria-supported vanadia. The effect of vanadia incorporation on the textural properties of samaria is briefly discussed. The adsorption of probe molecules and a cyclohexanol decomposition reaction have been adopted to explore the acid-base property of the system. The catalytic behavior of the supported system towards the oxidative dehydrogenation of ethylbenzene has also been studied.

The oxidative dehydrogenation of ethylbenzene is a reaction of much industrial importance owing to the commercial applications of styrene. Industrially, styrene is prepared by the alkylation of benzene using ethylene. Generally used catalyst systems for the preparation of styrene from ethylbenzene comprise $\text{SiO}_2\text{-Al}_2\text{O}_3$,^{8,9} V-Mg-O ,¹⁰ and $\text{SnO}_2\text{-P}_2\text{O}_5$ systems.¹¹ Among the various systems screened, V-Mg-O systems were found to be highly selective for the preparation of styrene.¹⁰

Experimental

1. Catalyst Preparation. $\text{Sm}(\text{NO}_3)_3$ (purity 99.9%) and NH_4VO_3 (purity 99.5%) were obtained from Indian Rare earth Ltd., Udyogamandal, Kerala, and S. D. Fine Chem. Ltd., Boisar, respectively. Samarium oxide was prepared through precipitation by a hydroxide method using a 1:1 ammonia solution.¹² Supported vanadia catalysts were prepared by the conventional wet impregnation method (excess solvent technique), as reported by Kanta Rao and co-workers.¹³ Catalysts with 0, 3, 7, 11, and 15 percentages of vanadia were prepared and designated as S, V3, V7, V11, and V15, respectively. The catalysts were sieved so as to obtain particles of mesh size < 100 microns. Prior to each experiment, the catalyst was activated in a current of dry air at 500 °C.

2. Catalyst Characterisation. **2.1. Analytical Data.** The chemical composition of the supported systems was determined by using energy-dispersive X-ray (EDX) analysis (Steaoscan 440 Cambridge, UK). Identification of different phases was done using a Rigaku D-Max C X-ray Diffractometer, with Ni-filtered $\text{Cu K}\alpha$ radiation ($\lambda = 1.5404 \text{ \AA}$). The mean crystallite size of the sample was determined from the broadening of the X-ray diffraction peak, following the Scherrer method. The FTIR spectra of the powder samples were recorded over the range 4000–400 cm^{-1} by the KBr disk method using a Shimadzu DR 8001 instrument. A Micromeritics Flowprep-060 instrument was used to determine the specific surface area by the BET method with nitrogen gas used as an adsorbate. The pore volume and pore-size distribution of the catalysts were measured by mercury

Table 1. Physico Chemical Characteristics of the Supported Systems

Catalyst	Percentage of vanadia	Crystallite size/nm	Surface area/m ² g ⁻¹	Pore volume /cm ³ g ⁻¹	Limiting amount adsorbed/mmol m ⁻²	
					TCNQ	Chloranil
Sm ₂ O ₃	0	19.94	20.78	1.41	5.50	4.37
V3	3.37	9.39	17.19	0.89	5.26	4.26
V7	6.85	9.63	21.91	0.64	3.84	3.32
V11	11.27	8.61	25.54	0.67	2.28	1.91
V15	14.59	6.51	25.48	0.59	2.25	1.87

porosimetry using Quantachrome, Auto scan-92 porosimetry (USA). The thermal stability of the samples was established by a TG-DTA analysis by using a Shimadzu TGA-50 instrument with a heating rate of 10 °C/min in a nitrogen atmosphere.

2.2. Acid Base Properties. 2.2.1 Electron Donating

Properties For determining the basicity of the system, adsorption studies of electron acceptors (EA) were performed using the following probe molecules: 7,7,8,8-tetracyanoquinodimethane (TCNQ) [Merk-Schuchandt], 2,3,5,6-tetrachoro benzoquinone (chloranil) [Sisco Research Laboratories Pvt. Ltd.], and *p*-dinitrobenzene (PDNB) [Merk-Schuchandt] with electron affinity values of 2.84, 2.40, and 1.77 eV, respectively. The following procedure was adopted for adsorption studies. Previously activated samples were stirred with a solution of EA in acetonitrile for 4 h in an airtight stirrer. The amount of the electron acceptor adsorbed on the catalyst surface was estimated from the difference in the concentration of EA in solution before and after adsorption, which was measured by means of a Shimadzu 160-A spectrophotometer (λ_{max} of the electron acceptors in acetonitrile are 393.5, 288, and 262 nm for TCNQ, chloranil, and PDNB, respectively). The adsorption isotherms were of the Langmuir type. From the Langmuir adsorption isotherms, the limiting amount of the electron acceptor adsorbed was obtained.

2.2.2 Temperature-Programmed Desorption (TPD) Studies. About 0.5 g of a pelletised sample was activated at 300 °C inside the reactor under nitrogen flow for 2 h. After cooling to room temperature, the sample was allowed to adsorb a definite amount of ammonia in the absence of a carrier gas, and the system was allowed to attain equilibrium. The excess and physisorbed ammonia was flushed out by a current of nitrogen, and under a controlled temperature program the amount of ammonia leached out was determined volumetrically.

2.2.3 Cyclohexanol Decomposition Reaction. The reaction was performed in a gas-phase silica reactor and the products were analysed by a GC fitted with a 6' × (1/8") stainless-steel column packed with 5% NPQSB + H₃PO₄ on anachrom A 80/100 mesh.

2.3. Catalytic Activity Study. Oxidative dehydrogenation of ethylbenzene was carried out in the vapor phase. Before each experiment, the catalyst was activated in a current of dry air at 500 °C, and then brought to the reaction temperature in the presence of a nitrogen flow. Ethylbenzene was then introduced into the carrier stream from a saturator containing liquid ethylbenzene. The mass balance was noted each time and liquid products were analyzed using a Shimadzu GC-15A gas chromatograph fitted with a xylene master capillary column and FID.

Results and Discussion

1. Catalyst Characterization. 1.1. Analytical Data.

Vanadia impregnation imparted a pale-yellow colour to the

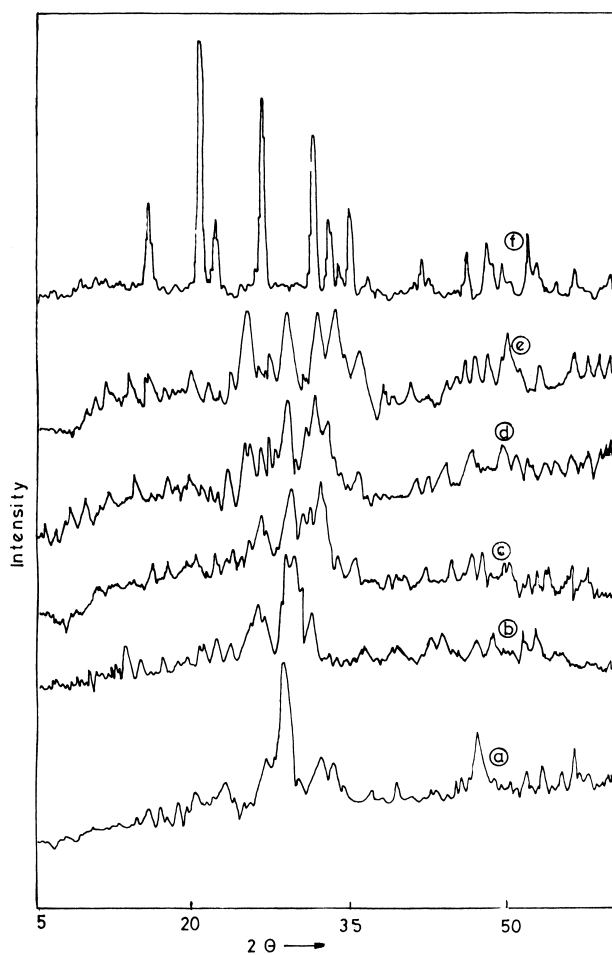


Fig. 1. X-ray diffraction patterns of catalysts (a) Sm₂O₃; (b) V3; (c) V7; (d) V11; (e) V15; (f) V₂O₅.

supported systems. The elemental composition of the supported system determined by an EDX analysis, is presented in Table 1. As revealed by the XRD patterns (Fig. 1), the intensity of the peaks became lowered, suggesting a decrease in the crystallinity of samaria as a result of vanadia incorporation, i.e., the interaction between V₂O₅ and the support hinders the transition of samaria from the amorphous phase to the crystalline phase. Prominent peaks due to crystalline samaria appeared at 2θ values of 28.0, 32.5, 48.0, and 55.5°. Additional peaks appeared at 2θ values of 18.6, 24.6, 31.0, 33.2, and 49.0°, which were identified to be due to samarium tetraoxovanadate. This agrees with the reports by Corma et al. that basic oxides preferably form compounds with vanadia.⁴ The rel-

ative intensity of the peaks supports a gradual increase of the samarium tetraoxovanadate percentage along with an increase in the vanadia content. The characteristic peaks of crystalline vanadia were not observed in the supported catalysts, even at higher loadings, due to the basic nature of samaria. The average crystallite size calculated by employing Scherrer's formula is given in Table 1.

The FTIR spectra of the supported systems are provided in Fig. 2. The spectra of the different vanadia-loaded systems were similar, except that the intensity of the bands due to vanadia was low in lower vanadia-loaded systems. For a comparison, the spectra of a V15 sample along with pure samaria and V_2O_5 are given in Fig. 3. The characteristic band at 1020 cm^{-1} due to V_2O_5 is not observed in the spectrum of the supported system thus confirming the results of an X-ray diffraction study. However, micro-crystals of V_2O_5 may be present, which cannot be detected by the X-ray diffraction pattern and

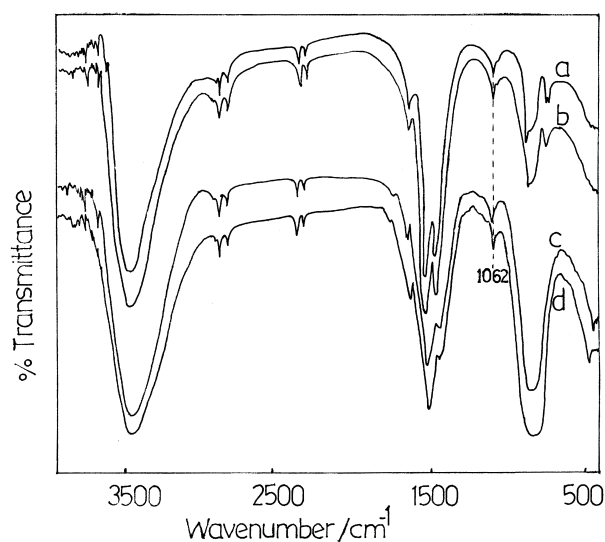


Fig. 2. FTIR spectra of the supported vanadia systems (a) V3; (b) V7; (c) V11; (d) V15.

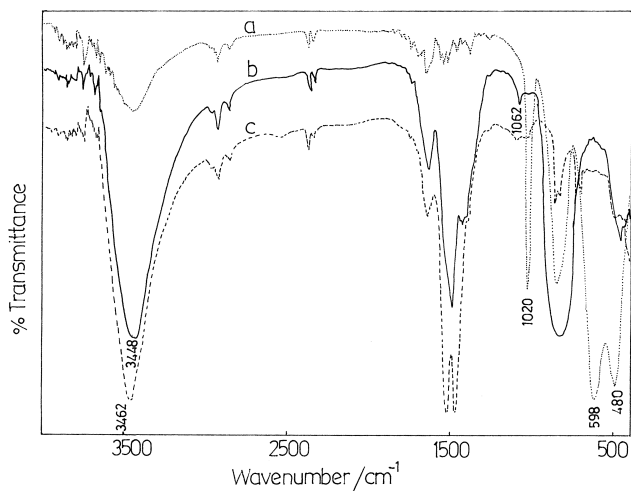


Fig. 3. FTIR spectra of (a) V_2O_5 ; (b) V15 system; (c) Sm_2O_3 .

an IR spectral analysis. The weak band at 1062.7 cm^{-1} is attributed to the $V=O$ stretching mode arising from the surface vanadium(IV) oxide species. The probability of dioxo structures in the surface species is ruled out, which when present exhibits several combination bands.¹⁴ Surface vanadia was identified as being an isolated species, since the polyvanadates exhibit $V=O$ stretching frequencies in the $1000\text{--}950\text{ cm}^{-1}$ region as suggested by Frederickson et al.¹⁵ The characteristic peaks due to vanadia are more clear in the DRIFT spectra given in Fig. 4. A tetrahedral geometry was assigned to isolated monooxo species, because it has been well established that isolated monooxo species exist as tetrahedral vanadium(IV) oxide units [$(O=V(O-M)_3$ type, where "M" is the support metal ion)] in the supported systems.¹⁶⁻¹⁸ The VO_4^{3-} entity that results from tetraoxovanadate justifies the presence of the broad band observed in the range $700\text{--}900\text{ cm}^{-1}$.¹⁹ A broad band typical for surface hydroxy groups was detected at around 3500 cm^{-1} . In the case of pure samaria, the corresponding broad band appeared at 3462 cm^{-1} , whereas for vanadia-loaded systems the above-mentioned band was located at 3448 cm^{-1} . Hence, it is plain that, while comparing with Sm_2O_3 , there is a shift of the band to lower frequency for the supported system. The IR band at higher frequency has been assigned to the most basic hydroxy group, and the decrease in frequency of the surface hydroxy group has been associated with increasing acidity.²⁰ Hence, the aforementioned shift indicates the participation of basic hydroxy groups in the bond formation with vanadia. In addition, this leads us to the conclusion that vanadia incorporation induces an enhancement of the Brønsted acidity.

A thermal-analysis curve exhibited two distinct weight losses, as confirmed by the DTG pattern. The initial weight loss in the $100\text{--}200\text{ }^\circ\text{C}$ region corresponds to a loss of physisorbed water. A further weight loss, which occurs in the $350\text{--}450\text{ }^\circ\text{C}$ range, accounts for the loss of surface hydroxy group due to a high percentage of rare earth oxide in supported samples. Besides, tetragonal tetraoxovanadate formation also takes place in this region, as reported by Oliveira and co-workers.²¹ The DTA profile for the supported system showed two endothermic peaks, supporting the above observation. Vanadia loss takes place only after $800\text{ }^\circ\text{C}$, indicating a high stability of the supported system.

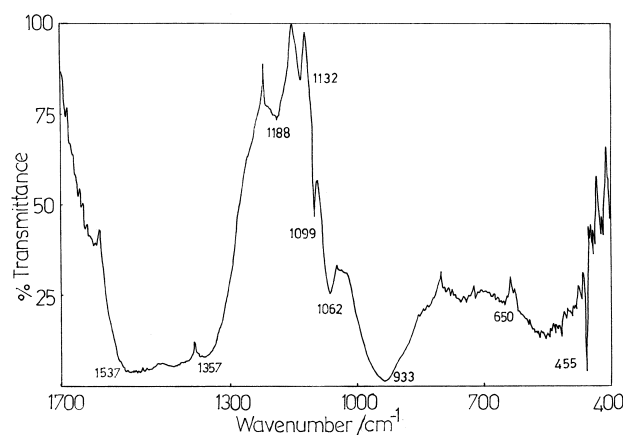


Fig. 4. Diffuse reflectance infrared (DR-IR) spectrum of V15 system.

From Table 1, it is apparent that there are no marked variations in the surface area, indicating that the impregnation procedure didn't appreciably affect the morphology of samaria. Still, there is an initial marginal loss, which can be accounted for by the reduction of pore radii of bigger pores, as evident from the pore-volume distribution curves. Further, vanadia addition prevents the agglomeration of particles, which leads to an enhancement of the surface area.

2. Acid Base Properties. 2.1. Ammonia TPD Studies.

Ammonia can be adsorbed on an oxide surface through hydrogen bonds or through dipolar interaction yielding the total acidity of the system (both Brønsted and Lewis type). Figure 5 shows acid-strength distribution profiles of pure samaria and supported analogues. The area of the peaks corresponds to the acid amount in that particular temperature range. As evident from the figure, pure samaria possesses a small amount of weak acid sites and an appreciable amount of strong acid sites. Vanadia impregnation increased the amount of ammonia desorbed at a lower temperature region, whereas a considerable reduction is noticed concerning the amount of ammonia desorbed at higher temperatures. It is generally accepted that evacuation of metal oxide surfaces at 400 °C removes most of the adsorbed probe molecules from the Brønsted acid sites.^{22,23} In the present case, the amount of ammonia desorbed up to 300 °C is taken as a measure of the Brønsted acidity. The amount of ammonia desorbed at higher temperatures is considered to be due to ammonia bound on Lewis acid sites.

A gradual decrease in the amount of Lewis acidity along with an increase of the vanadia percentage is evident from the TPD curves. According to Kantcheva et al., sites responsible for Lewis-type acidity are coordinately unsaturated cations of the support.²⁴ Hence, it is obvious that Lewis acid sites resulting from the exposed cations of samaria are being utilized for the formation of bonds with vanadia, as reported by Das et al.¹⁶ Besides, the figure reveals that the incorporation of V₂O₅ remarkably increases the concentration of Brønsted acid sites, which is consistent with earlier reports.^{25,14} This is also in agreement with the conclusions derived from the FTIR spectra, which predicted an increase of acidic hydroxy groups. Turek

et al. proposed a crowding effect of the supported species as a necessary condition for the generation of Brønsted acidity at higher vanadia loadings.²⁶ They attributed Brønsted acid sites at high vanadia loadings to an increase in the surface density of molecularly dispersed species. According to them, the simplest conceivable model of the Brønsted acid site that can be proposed here consists of two surface species sharing a common H⁺ located between two oxygen atoms belonging to two different V–O–M groups. Brønsted acidity is created independent of the structure of H⁺ connected surface metal oxide units, if they are in a privileged configuration to each other. However, from the figure, it is clear that no considerable change in the amount of Brønsted acid sites is found as the weight percentage of vanadia is increased from 3 to 15. This implies that the crowding effect might have been reached by the addition of 3 wt% vanadia, itself. Further, vanadia addition may be primarily contributing towards samarium tetraoxovanadate.

2.2. Electron-Donating property—Measure of Lewis Basicity.

The utility of electron acceptor adsorption for studying the electron-donating property has been well established,^{27–29} which provides useful information regarding the Lewis basicity of the catalysts. In this method, the strength and distribution of basic sites are followed by the adsorption of electron acceptors (EA). The electron-donating capacity depends on the nature of the donor sites and the electron affinity of the electron acceptors used. The extent of electron transfer decreases along with a decrease in the electron affinity value of the electron acceptor. An electron acceptor with a high electron affinity value become adsorbed on both weak and strong donor sites, while the adsorption of EA with low electron affinity occurs only at strong basic sites.

For supported systems, PDNB adsorption was too negligible, indicating the absence of very strong basic sites. Electron-donor adsorption imparted characteristic coloration to the catalyst surface, suggesting the formation of radical anions. On pure Sm₂O₃, TCNQ adsorption developed a bluish-green color and chloranil developed a pale-pink color. In the case of supported catalysts, which were pale-yellow colored, the colors generated were pale-green and pale-grey, respectively. The limiting amount of electron acceptors, which is a measure of the Lewis basicity, can be determined from the Langmuir plot (Fig. 6). Since TCNQ is a stronger EA, leading to adsorption on both weak and strong donor sites, the limiting amount adsorbed was higher in the case of TCNQ adsorption, while the limiting amount adsorbed for chloranil was low (Table 1). A survey of the limiting amount adsorbed clearly indicates that the basicity shows a decreasing trend with a progressive addition of vanadia. A similar observation as a result of vanadia addition was reported by Le Bars and co-workers.³⁰ It was accepted by earlier workers that the factors responsible for the electron-donating capacity are surface hydroxy ions and surface O²⁻ centers. At higher activation temperatures, trapped electron centers also function as electron donor sites.^{31,32} However, it has been reported that, electron-defect centers are created only at an activation temperature above 500 °C.³³ Thus the present case, a major contribution towards basic sites arises from surface hydroxide ions resulting from the addition of vanadia. A decreasing amount of the electron acceptor adsorbed

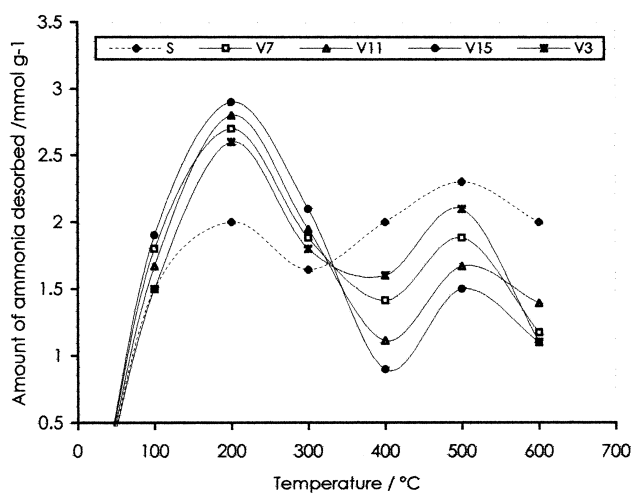


Fig. 5. Temperature programmed desorption curves of ammonia over Sm/V catalysts.

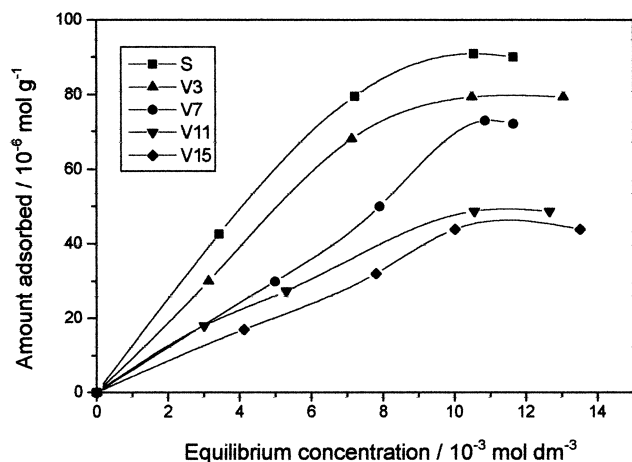


Fig. 6. Langmuir adsorption isotherms of chloranil over Sm/V systems.

accounts for the decrease in the surface hydroxide ions as a result of vanadia addition. Supporting evidence for this conclusion is obtained from the FTIR spectra of the supported systems, where a shift for the hydroxy band position was noticed.

2.3. Cyclohexanol Decomposition Reaction. The influence of vanadia loading on the acid-base properties have been confirmed through studies on the decomposition of cyclohexanol over the supported system (Table 2). The amphoteric character of the alcohol permits its interaction with acidic and basic sites, leading to the formation of cyclohexanol and cyclohexanone. Both acid and base sites participate in dehydrogenation, whereas dehydration takes place with the intervention of acid sites. Hence, the dehydrogenation rate/selectivity of cyclohexanone is proportional to both the acidity and basicity, whereas the dehydration rate/selectivity of cyclohexene is found to be proportional to the acidity.³⁴ Vanadia addition

brings about a dramatic improvement in the selectivity of dehydration products, which were catalyzed by Brønsted acid sites, as reported by Bezouhanava et al.³⁵ An enhancement of the Brønsted acidity by vanadia incorporation is apparent from these data. Further, the reduced selectivity of cyclohexanone on a supported system indicated a decrease in both the acid and base sites which take part in dehydrogenation. These observations lend support to a proposed decrease of Lewis acid and base sites with a concomitant increase of Brønsted acid sites, as concluded from the adsorption of probe molecules. Moreover, from the results presented in Table 2, it is clear that there is no remarkable change in the selectivity of dehydration products as the composition of vanadia varies from 3 to 15 wt%, thus substantiating the role of vanadia in vanadate formation at higher concentrations.

3. Catalytic Activity Studies. The effect of vanadia on the catalytic performance towards the oxidative dehydrogenation (ODH) of ethylbenzene is given in Table 3. Along with styrene, small amounts of benzene, toluene, and carbon oxides are also detected among the products. The conversion of ethylbenzene showed a gradation with the vanadia content in the system. The selectivity towards styrene was too poor for pure vanadia, which catalyzed almost the complete oxidation of ethylbenzene, as evident from the greater percentage of carbon oxides. From the ODH data, it is obvious that selective oxidation activity is greatly influenced by the supporting vanadia. The styrene selectivity was almost constant at a higher vanadia percentage, and was found to be independent of the percentage conversion. The selectivity of toluene and benzene were decreased with the concentration of vanadia in the supported catalysts. The reaction was also performed over pure SmVO_4 . Pure SmVO_4 exhibited negligible activity due to an extremely small surface area ($9.26 \text{ m}^2/\text{g}$), though the system was fairly selective.

Table 2. Cyclohexanol Decomposition Data over Sm/V Catalyst System

Catalyst	Conversion/%	Product distribution/%			Selectivity/%	
		MCP	Cyclohexene	Cyclohexanone	C=C	C=O
Sm_2O_3	40.85	—	10.95	29.90	26.81	73.19
V3	38.61	1.19	33.73	3.69	90.44	9.56
V7	39.59	2.12	34.09	3.38	91.46	8.54
V11	42.40	3.43	35.76	3.21	92.42	7.58
V15	43.07	3.63	36.34	3.10	92.80	7.20

Reaction conditions: catalyst = 2.5 g; reaction temp = 300 °C; feed rate = 6 mL/h, time on stream = 1 h.

Table 3. Oxidative Dehydrogenation of Ethylbenzene over Sm/V System

Catalyst	Conversion/%	Selectivity/%			
		Styrene	Toluene	Benzene	C-oxides
V_2O_5	35.8	5.2	1.6	3.0	90.2
V3	8.1	77.0	3.9	3.1	16.0
V7	13.8	86.7	2.7	3.0	9.6
V11	14.9	87.3	1.3	1.3	10.1
V15	16.6	86.6	1.2	0.9	10.4

Reaction conditions: reaction temperature: 475 °C; feed rate: 6 mL/h; catalyst: 2 g; time on stream: 1 h; air flow rate: 20 mL/min.

3.1. Selective Oxidation Activity of the Supported System. The selective oxidation activity of the supported vanadia system is evident from Table 3. The behavior of vanadia-based systems in selective oxidation strongly depends on the redox property of the vanadium species as well as on the acid base character of the support and catalyst.^{36,37} Tagawa et al. observed that the acid sites of the Hammett H_o values between 1.5 and -5.6 are active for ethylbenzene conversion, which adsorb ethylbenzene reversibly. Oxidation of the same occurs on the basic sites of pK_a lying between 17.2 and 26.5.⁹ However, in Sm/V systems, no such sites were detected by the Hammett indicator method, leading to the conclusion that the influence of the acid base properties on the selective oxidation activity is negligible in the present case. Hence, apart from the acido basic properties, the redox property plays an important role in selective oxidation over Sm/V catalyst systems.

According to Sachtler et al.,^{38,39} the selectivity in the oxidation reaction is determined by two factors: 1) by the intrinsic activity of lattice oxygen and 2) by their availability. The intrinsic activity depends on the nucleophilicity of the lattice oxygen, which was proposed as a site capable of abstracting hydrogen atoms as hydrogen ions.⁴⁰ This in turn depends on the coordination environment of the vanadium ion in the supported system. Grzybowska et al. have shown that the V^{5+} ion exists in isolated VO_4 tetrahedra and tetraoxovanadates.⁷ It is accepted that vanadia in a tetrahedral coordination is most active in oxidative dehydrogenation.^{4, 41–44} For the present system, both species having a tetrahedral geometry, this condition is satisfied, indicating tetrahedral vanadia as the active species present in the supported system. Oxygen attached to a V^{5+} in tetrahedral coordination is found to be highly nucleophilic.⁷

Another factor on which the selectivity depends is the availability of lattice oxygen at the reaction site, which is expressed as the average number of oxygen molecules that react with each hydrocarbon molecule (also termed as average oxygen stoichiometry, AOS).⁴¹ The number of vanadium(IV) oxide units that can effectively interact with the adsorbed hydrocarbon unit determines the AOS in the case of a particular supported system. If only a limited number of lattice oxygens are available, the oxidation stops at a particular level, resulting in partial oxidation products. V_2O_5 has a layer structure, and all of the layers take part in the oxidation reaction because the diffusion of oxygen from other layers of the lattice is much faster in V_2O_5 ,⁴⁵ leading to complete oxidation. In the case of a supported vanadia system, there is no large reservoir of bulk oxygen available to abstract so many oxygens. In the present case, VO_4 units are isolated (sufficiently apart), which supplies only a limited number of oxygen atoms to react with a hydrocarbon

molecule, thus improving the selectivity. Consequently, the locally limited amount of reactive lattice oxygen might be an explanation for the selective oxidation activity of the Sm_2O_3/V_2O_5 system.

As shown in Table 3, above 3% vanadia, the styrene selectivity was almost constant for the supported system. This can be explained based on the preferential formation of $SmVO_4$ at higher vanadia percentages. Up to 7% vanadia, surface species may contribute to the styrene selectivity. The completion of monolayer coverage occurs at about 7% vanadia. At higher vanadia concentration, vanadate has a prominent role, which exhibits a constant selectivity towards styrene, which is in accordance with Chang et al., who reported constant styrene selectivity for tetraoxovanadates.¹⁰

The interaction of ethylbenzene with acidic and basic centres of the catalyst surface resulted in the production of benzene and toluene. Wang et al. suggested that strong acidic sites could abstract α -hydrogen of ethylbenzene, thus facilitating the formation of benzene.⁴⁶ The decrease in the benzene selectivity with an increase in the vanadia content can be rationalized in terms of the reduction of strong acid sites, which has also been confirmed through ammonia desorption studies. Likewise, Krause proposed the role of strong basic sites for toluene formation.⁴⁷ Strong basic sites on a catalyst preferably abstract beta hydrogen, leading to a cleavage of the C–C bond of the side chain resulting in a high yield of toluene. According to the results obtained from electron-donor property studies, the number of strong basic sites is becoming reduced due to vanadia impregnation. The expected decrease of the toluene percentage is consistent with the results presented in Table 3.

3.2. Effect of the Reaction Temperature. V7 is taken as a representative of a supported system to examine the effect of various reaction parameters on the activity and selectivity of the catalysts. ODH of ethylbenzene was performed at different temperatures over V7 to understand the effect of the reaction temperature on the system. The dependence of the catalytic activity on the reaction temperature is given in Table 4. There was an enhancement in the conversion of ethylbenzene as the temperature was increased from 475 to 525 °C. However, no remarkable change in the selectivity of styrene was observed over the above temperature range. A similar observation was also found with magnesium orthovanadate in the ODH of ethylbenzene.¹⁰

3.3. Effect of Flow Rate. In another series of experiments, the effect of the contact time on the catalytic activity and the selectivity of products was studied. The activity and selectivity variations as a function of the feed rate over V7 are shown in Fig. 7. The conversion decreased along with an in-

Table 4. Influence of Reaction Temperature on Conversion and Selectivity

Temperature/°C	Conversion/%	Selectivity/%			
		Styrene	Toluene	Benzene	C-oxides
475	13.1	84.6	2.7	3.0	9.7
500	18.0	85.0	2.0	3.0	10.0
525	24.0	83.3	1.2	3.5	12.0

Reaction conditions: catalyst, V7:2 g; flow rate: 6 mL/h; time on stream: 1 h; air flow rate: 20 mL/min.

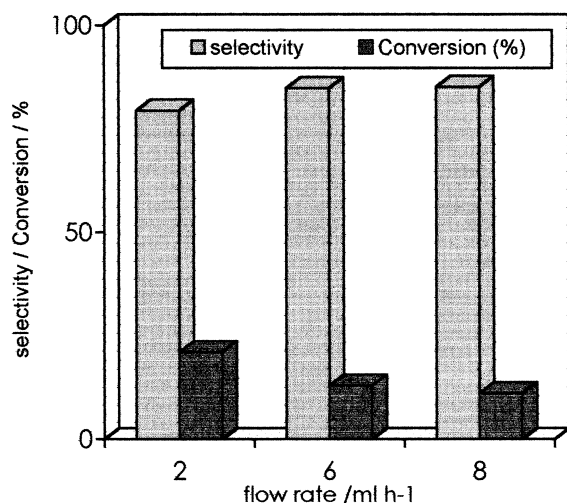


Fig. 7. Effect of flow rate on the conversion of ethylbenzene and selectivity of styrene.

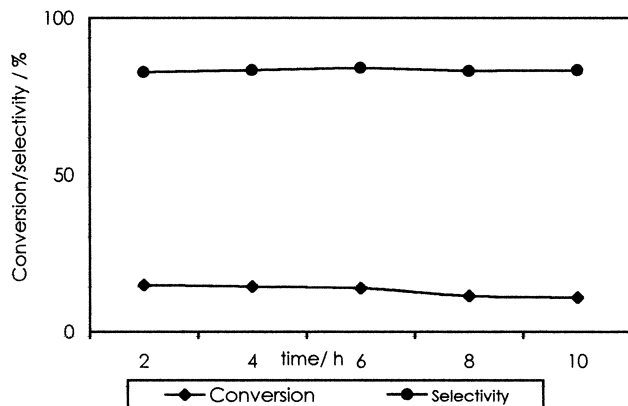
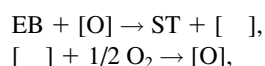


Fig. 8. Deactivation studies conducted over V7.

crease in the feed rate i.e., at a low contact time. The selectivity towards styrene was increased along with an increase in the feed rate. A small feed rate would increase the residence time of the reactant on the catalyst surface. A high conversion of ethylbenzene at higher contact times (small feed rates) can be attributed to the higher probability of the reactive adsorption. The possibility of product readsorption and the production of more oxygenated products are probable at low flow rates, which leads to less selectivity, as is evident from the figure. This is of prime importance while considering the highly mobile lattice oxygen of samaria, which replenishes the consumed oxygen at the reaction site, leading to a high percentage of carbon oxides.

3.4. Deactivation Study. Time-on-stream studies were conducted on V7 to establish the stability of the supported catalysts. The results are shown in Fig. 8. The conversion was more or less constant, although a slight deactivation was observed after 6 h. The selectivity also remained unaltered during a prolonged treatment with reactants. The catalyst turned dark grey after continuous use, probably due to carbon deposits and a reduction of the catalyst. The original color could be regained by treating the catalyst in flowing air at 400 °C for 2 h.

3.5. Mechanism. In the oxidative dehydrogenation of ethylbenzene, one of the most probable suggested mechanisms, consists of an abstraction of "H" from the ethylbenzene by the lattice oxygen to form styrene, and a reoxidation of the catalyst by gas-phase oxygen.⁴⁸ Similar conclusions regarding the mechanism have been reached by Tagawa et al.⁹ To obtain insight into the reaction pathway over Sm/V systems, the reaction was carried out in the absence of air (Table 5). The fact that the catalytic activity and percentage conversion were significantly reduced under non-oxidative conditions pointed out to the role of gaseous oxygen in the reaction. The reason for the reduced conversion may be a reduction of the catalyst. The formation of styrene reduces the catalyst system, and the possibility of reoxidation is limited under non-oxidative conditions. The presence of air increases the conversion, which indicates that the presence of gaseous oxygen favors the redox operation of the catalyst by supplying oxygen needed for hydrogen abstraction by reoxidising the catalyst. Hence, the aforesaid mechanism (Mars and van Krevelen) may be operating here, which can be represented as



where [O] is the lattice oxygen and [] is the lattice vacancy.

The oxygen-supplying entity in the case of the ODH reaction is a matter of conflict, even now. Several oxygen species were suggested as the "H" abstracters, including terminal V=O, bridging oxygen of M–O–V bond, and Brønsted acid sites.⁷ However, studies conducted on alumina exclude V=O from the list, since such an active site is not necessary to create an active site.⁷ This is supported by the fact that the activity and selectivity do not vary much with the percentage of vanadia, even though the V=O species at higher and lower vanadia-loaded systems differ widely. According to reports, it is the highly nucleophilic bridging oxygen that furnishes active and selective sites in the case of tetraoxovanadate systems, in general. Hence, the possibility of bridging oxygen acting as the

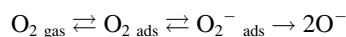
Table 5. Dehydrogenation of Ethylbenzene over Sm/V System

Catalyst	Conversion/%	Selectivity/%			
		Styrene	Toluene	Benzene	C-oxides
V3	6.4	82.9	9.8	2.8	4.6
V7	6.8	90.8	4.0	1.4	3.7
V11	7.2	90.0	4.0	1.5	3.4
V15	7.5	87.9	4.0	1.8	3.2

Reaction conditions: reaction temperature: 475 °C; feed rate: 6 mL/h; catalyst, V7: 2 g; time on stream: 1 h.

active species that abstract the hydrogen from ethylbenzene is tentatively suggested for the present system. This explains the negligible activity variation with the increase of vanadia composition in the supported system. The formation of amorphous vanadium(IV) oxide entities might not increase with the percentage of vanadia. However, the probability of Brønsted sites as the active sites cannot be ruled out here, since it was observed from ammonia desorption studies that vanadia addition enhances the Brønsted acidity from TPD studies using ammonia.

In the ODH of ethylbenzene, the activation of a C–H bond should be considered first, which is often regarded as the rate-determining step.⁹ In the activation of hydrocarbons containing π electrons, the abstraction of H atoms on an oxide centre is facilitated by the donation of π electrons to a Lewis site, which leads to a weakening of the C–H bond (allylic type oxidation). The oxygen in the catalyst abstracts the H in ethylbenzene. The hydrocarbon activation centre is thus considered to be a couple of $M^{n+}-O$, which is regarded as an acid-base pair. Reduced vanadium ions chemisorb gaseous oxygen reversibly, and are converted to lattice O^{2-} . The dissociation of molecular oxygen with electron transfer according to overall reaction is shown below.^{49,50}



It is clearly apparent from Table 5 that the selectivity towards styrene is increased under non-oxidative reaction conditions, revealing that gaseous oxygen participates in the non-selective oxidation of hydrocarbons. The decrease of the styrene selectivity in the presence of air may not be due to an increase of the ethylbenzene conversion, because the styrene selectivity does not depend on the conversion. An alternative suggestion for the high styrene selectivity under the non-oxidative condition is the absence of gaseous oxygen. A reduction of the styrene selectivity in the presence of gaseous oxygen is also reported by Chang et al.¹⁰ Yang et al.⁵¹ and Shakhnovich et al.⁵² also proposed a similar degradation of the dehydrogenation product by gaseous oxygen.

Conclusion

Vanadate species both in amorphous and crystalline forms were formed by supporting vanadia on samaria by wet impregnation. Surface vanadia existed as tetrahedral units in the supported system. Lewis acid and base sites of the support were reduced upon vanadia incorporation, concomitant with an enhancement of the Brønsted acid sites. Surface studies using different experimental methods indicated the participation of basic OH groups and Lewis-acid sites of the support in bond formation with vanadia species. Vanadia created redox sites on samaria. In the oxidation of ethylbenzene, the activity for partial oxidation was enhanced through supporting vanadia on samaria. Vanadium ion in tetrahedral coordination was found to be selective towards styrene, and the active site was concluded to be the bridging oxygen of the surface vanadium(IV) oxide species. The higher vanadia-loaded systems exhibited constant styrene selectivity, where crystalline tetraoxovanadates were predominantly formed.

The authors wish to acknowledge their sincere gratitude to CSIR, New Delhi for the award of SRF to N. K. Renuka and AICTE (New Delhi) for the financial assistance.

References

- 1 C. J. Ottamari and A. Anderson, *Catal. Today*, **3**, 211 (1988).
- 2 T. J. Dines, C. H. Rochester, and A. M. Wars, *J. Chem. Soc., Faraday Trans.*, **87**, 1473 (1991).
- 3 J. M. Lopez-Nieto, G. Kremenik, and J. G. Fiero, *Appl. Catal.*, **61**, 235 (1990).
- 4 A. Corma, J. M. Lopez-Neito, N. Paredes, M. Perez, Y. Shen, H. Cao, and S. L. Suib, *Stud. Surf. Sci. Catal.*, **72**, 213 (1992).
- 5 Y. Nagakawa, T. Ono, H. Miyata, F. J. Hatayama, and Y. Kubokawa, *J. Chem. Soc., Faraday Trans.*, **1**, **79**, 2929 (1983).
- 6 H. Miyata, M. Kohno, T. Ohno, F. J. Hatayama, and Y. Kubokawa, *J. Chem. Soc., Faraday Trans.*, **1**, **85**, 3663 (1989).
- 7 B. Grzybowska-Swierkosz, *Appl. Catal. A: Gen.*, **157**, 409 (1997).
- 8 T. Tagawa, T. Hattori, and Y. Murakami, *J. Catal.*, **75**, 56 (1982).
- 9 T. Tagawa, T. Hattori, and Y. Murakami, *J. Catal.*, **75**, 66 (1982).
- 10 W. S. Chang, Y. Z. Chen, and B. L. Yang, *Appl. Catal. A: Gen.*, **124**, 221 (1995).
- 11 Y. Murakami, K. Iwayama, H. Uchida, T. Hattori, and T. Tagawa, *J. Catal.*, **71**, 257 (1981).
- 12 "Encyclopedia of Industrial Chemical Analysis," ed by F. D. Snell and L. S. Ettre, Interscience, New York (1973), Vol. 17, p. 475.
- 13 K. V. Narayana, A. Venugopal, K. S. Rama Rao, V. Venkat Rao, S. Khaja Masthan, and P. Kanta Rao, *Appl. Catal. A*, **150**, 269 (1977).
- 14 I. E. Wachs, *Catal. Today*, **27**, 437 (1996).
- 15 L. D. Frederickson, Jr. and D. M. Hausen., *Anal. Chem.*, **35**, 818 (1963).
- 16 N. Das, H. Eckert, H. Hu, I. E. Wachs, J. Walcer, and F. Fehre, *J. Phys. Chem.*, **97**, 8240 (1993).
- 17 H. Eckert and I. W. Wachs, *J. Phys. Chem.*, **93**, 6796 (1989).
- 18 Xingtao Gao, J. L.G. Fierro, and I. E. Wachs, *Langmuir*, **15**, 3169 (1999).
- 19 J. A. Gadsden, "IR Spectra of Minerals and Related Compounds," (1975), p. 26.
- 20 H. P. Boehm and H. Knozinger, "Catalysis," ed by J. R. Anderson and M. Moudart, Springer, Berlin (1983), Vol. 4, Chap. 2.
- 21 H. P. Oliveira, F. J. Anaissi, and H. E. Toma, *Mat. Res. Bull.*, **33**, 1783 (1998).
- 22 A. Auroux and A. Gervasini, *J. Phys. Chem.*, **94**, 6371 (1990).
- 23 F. Hatayama, T. Ohno, T. Maruoka, T. Ono, and H. Miyata, *J. Chem. Soc., Faraday Trans.*, **87**, 2629 (1991).
- 24 M. M. Kantcheva, K. I. Hadjiivanov, and D. G. Klissurski, *J. Catal.*, **134**, 299 (1992).
- 25 J. R. Sohn, S. G. Cho, Y. I. Pae, and S. Hayashi, *J. Catal.*, **159**, 170 (1996).
- 26 A. M. Turek, I. E. wachs, and E. De Canio, *J. Phys. Chem.*, **96**, 5000 (1992).
- 27 K. Esumi and K. Meguro, *J. Colloid Interface Sci.*, **66** (1),

- 192 (1978).
- 28 S. Sugunan and G. D. Rani, *J. Mat. Sci. Lett.*, **10**, 887 (1991).
- 29 R. P. Porter and W. K. Hall, *J. Catal.*, **5**, 366 (1966).
- 30 J. Le Bars, J. C. Vedrine, A. Auroux, S. Trautman, and M. Baerns, *Appl. Catal. A: Gen.*, **119**, 341 (1994).
- 31 K. Esumi and K. Meguro, *J. Adhesion Sci. Technol.*, **4**, 393 (1990).
- 32 K. Meguro and K. Esumi, *J. Colloid Interface Sci.*, **59** (1), 93 (1977).
- 33 B. D. Flockhart, I. R. Leith, and R. C. Pink, *Trans. Faraday Soc.*, **65**, 542 (1969).
- 34 Mamoru Ai, *Bull. Chem. Soc. Jpn.*, **50**, 2579 (1997).
- 35 C. P. Bezouhanava and M. A. Al-Zihari, *Catal. Lett.*, **11**, 245 (1991).
- 36 T. Blasco and J. M. Lopez-Nieto, *Appl. Catal. A: Gen.*, **157**, 117 (1997).
- 37 E. A. Mamedov and V. Cortes-Corberan, *Appl. Catal. A: Gen.*, **127**, 1 (1995).
- 38 W. M. H. Sachtler and N. H. De Boer, "Proceedings 3rd International Congress on Catalysis, Amsterdam, 1964," Wiley, New York (1965), p. 240.
- 39 W. M. H. Sachtler, G. J. H. Dorgelo, J. Fahrenfort, and R. J. H. Voorhoev, "Proceedings 4th International Congress on Catalysis, Moscow, 1968," ed by B. A. Kazanski, Adler, New York (1968), p. 454.
- 40 A. Bielski and J. Haber, "Oxygen in Catalysis," Marcel Dekker, New York, NY (1991).
- 41 H. H. Kung and M. C. Kung, *Appl. Catal. A: Gen.*, **157**, 105 (1997).
- 42 J. G. Eon, R. Olier, and J. C. Volta, *J. Catal.*, **145**, 318 (1994).
- 43 T. Blasco, A. Galli, J. M. Lopez-Nieto, and F. Trifiro, *J. Catal.*, **169**, 203 (1997).
- 44 D. Patel, P. J. Andersen, and H. H. Kung, *J. Catal.*, **125**, 132 (1990).
- 45 C. Doornkamp, M. Clement, X. Gao, G. Deo, I. E. Wachs, and V. Ponec, *J. Catal.*, **185**, 415 (1999).
- 46 I. Wang, W. S. Chang, R. J. Sheiu, J. C. Wu, and C. S. Chang, *J. Catal.*, **83**, 438 (1983).
- 47 A. Krause, *Sci. Pharm.*, **38**, 266 (1970).
- 48 J. Hanuza and B. Jezowska-Trzebiatowska, *J. Mol. Catal.*, **4**, 271 (1978).
- 49 J. H. Lunsford, *Catal. Rev.*, **8**, 135 (1973).
- 50 A. Beilanski and J. Haber, *Catal. Rev.*, **19**, 1 (1979).
- 51 B. L. Yang and H. H. Kung, *J. Catal.*, **77**, 410 (1982).
- 52 G. V. Shakhovich, I. P. Belomestnykh, N. V. Nekrasov, M. M. Kostyukovsky, and S. L. Kiperman, *Appl. Catal.*, **12**, 23 (1984).